

The dielectric-coated conducting sphere excited in the symmetric transverse magnetic mode—resonant characteristics

PARVEEN WAHID AND R. CHATTERJEE

Department of Electrical Communication Engineering, Indian Institute of Science, Bangalore 560 012

Received on July 13, 1979.

Abstract

The complex resonant frequencies have been determined for a few TM_{en} modes by solving the characteristic equation obtained by using boundary value methods. The real part of the resonant frequency is lower for large values of the inner radius and decreases with increase in dielectric coating thickness for any particular mode. The imaginary part of the resonant frequency is found to increase with increase in coating thickness for a particular mode. The Q of the resonator has been computed at the real resonant frequency. The effect on the Q values by considering, (i) the energy loss due to radiation only, (ii) the energy loss due to radiation and the dielectric, (iii) the energy stored in the dielectric only and (iv) the energy stored in the dielectric and in the reactive field has been studied.

Key words : Dielectric-coated metal resonator, complex resonance frequency.

1. Introduction

The electromagnetic resonances of free dielectric samples have been the subject of study since the last few years¹⁻⁴. Resonators made of high dielectric constant materials with a low dissipation factor have high Q values and have many different applications.

In this paper, the resonant characteristics of the dielectric-coated conducting sphere have been studied by solving the characteristic equation obtained by using boundary value methods. The peak energy stored, the dielectric loss, the power loss by radiation and hence the Q values of the resonator have been studied theoretically.

2. Characteristic equation

Figure 1 of ref. 5 shows the geometry of the structure. The dielectric-coated conducting sphere is excited in the symmetry TM mode by a delta-function electric field source $E_0 e^{-j\omega t}$ applied normally over an annular ring of radius $b \sin \theta_1$ and width $(b - a) \sin \theta_1$, assuming that $(b - a) \ll a$ and $\ll b$. Let the delta-function E_0 have components E_r and E_θ , in the r and θ directions respectively, and be given by

$$E_0 = -\frac{V}{b \Delta \theta \sin \theta_1} \quad \text{for } \theta_1 - \frac{\Delta \theta_1}{2} < \theta < \theta_1 + \frac{\Delta \theta_1}{2} \quad (1)$$

$$E_0 = 0 \quad \text{for } \theta < \theta_1 - \frac{\Delta\theta_1}{2} \quad \text{and} \quad \theta > \theta_1 + \frac{\Delta\theta_1}{2} \quad (2)$$

where V is the excitation voltage applied across the gap $b \Delta \theta \sin \theta_1$ over the annular ring. The field components are⁵

Region $a \leq r \leq b$:

$$E_r^i = - \sum_n n(n+1) P_n(\cos \theta) \frac{1}{k_1 r} [L_{on} j_n(k_1 r) + M_{on} y_n(k_1 r)] e^{-j\omega t} + E_{r0} \quad (3)$$

$$E_\theta^i = - \sum_n P'_n(\cos \theta) \frac{1}{k_1 r} [L_{on} [k_1 r j_n(k_1 r)]' + M_{on} [k_1 r y_n(k_1 r)]'] e^{-j\omega t} + E_{\theta0} \quad (4)$$

$$H_\phi^i = \frac{k_1}{j\omega\mu_1} \sum_n P'_n(\cos \theta) [L_{on} j_n(k_1 r) + M_{on} y_n(k_1 r)] e^{-j\omega t}. \quad (5)$$

Region $r \geq b$:

$$E_r^e = - \sum_n n(n+1) N_{on} P_n(\cos \theta) \frac{h_n^{(1)}(k_0 r)}{k_0 r} e^{-j\omega t} \quad (6)$$

$$E_\theta^e = - \sum_n P'_n(\cos \theta) N_{on} \frac{1}{k_0 r} [k_0 r h_n^{(1)}(k_0 r)]' e^{-j\omega t} \quad (7)$$

$$H_\phi^e = - \sum_n \frac{k_0}{j\omega\mu_0} P'_n(\cos \theta) N_{on} h_n(k_0 r) e^{-j\omega t} \quad (8)$$

where

$$k_1 = \omega \sqrt{\mu_1 (\epsilon_1 + j \frac{\sigma_1}{\omega})} \quad \text{and} \quad k_0 = \omega \sqrt{\mu_0 (\epsilon_0 + j \frac{\sigma_0}{\omega})},$$

ω -angular frequency, $P_n(\cos \theta)$ is the Legendre polynomial, $j_n(k_1 r)$, $y_n(k_1 r)$ and $h_n^{(1)}(k_0 r)$ are the spherical Bessel, Neumann and Hankel function of the first kind respectively. L_{on} , M_{on} and N_{on} are the amplitude coefficients.

Applying the boundary conditions:

$$E_\theta^e = E_\theta^i \quad \text{and} \quad H_\phi^e = H_\phi^i \quad \text{at} \quad r = b \quad \text{and} \quad E_\theta^i = 0 \quad \text{at} \quad r = a; \quad (9)$$

we obtain the equations⁶

$$\begin{aligned} \frac{1}{k_1 b} [L_{on} [k_1 b j_n(k_1 b)]' + M_{on} [k_1 b y_n(k_1 b)]'] + \frac{C_{on}(b)}{k_1} \\ = N_{on} \frac{1}{k_0 b} [k_0 b h_n^{(1)}(k_0 b)]' \end{aligned} \quad (10)$$

$$\frac{k_1}{\mu_1} [L_{en} j_n(k_1 b) + M_{en} y_n(k_1 b)] = \frac{k_0}{\mu_0} N_{en} h_n^{(1)}(k_0 b) \quad (11)$$

and

$$\frac{1}{k_1 a} [L_{en} [k_1 a j_n(k_1 a)]' + M_{en} [k_1 a y_n(k_1 a)]' + \frac{C_{en}(a)}{k_1}] = 0. \quad (12)$$

Let z_n be the determinant of the coefficients of the amplitude coefficients, i.e.,

$$z_n = \begin{vmatrix} \frac{1}{k_1 b} [k_1 b j_n(k_1 b)]' & \frac{1}{k_1 b} [k_1 b y_n(k_1 b)]' & -\frac{1}{k_0 b} [k_0 b h_n^{(1)}(k_0 b)]' \\ \frac{k_1}{\mu_1} j_n(k_1 b) & \frac{k_1}{\mu_1} y_n(k_1 b) Y & -\frac{k_0}{\mu_0} h_n^{(1)}(k_0 b) \\ \frac{1}{k_1 a} [k_1 a j_n(k_1 a)] & \frac{1}{k_1 a} [k_1 a y_n(k_1 a)] & 0 \end{vmatrix} \quad (13)$$

Then, the condition $z_n = 0$, leads to the characteristic equation given below:

$$\frac{\left\{ \frac{[k_1 b j_n(k_1 b)]'}{k_1 b} \frac{[k_1 b y_n(k_1 a)]'}{k_1 a} - \frac{[k_1 b y_n(k_1 b)]'}{k_1 b} \frac{[k_1 b j_n(k_1 a)]'}{k_1 a} \right\}}{\left\{ k_1 j_n(k_1 b) \frac{[k_1 a y_n(k_1 a)]'}{k_1 a} - k_1 y_n(k_1 b) \frac{[k_1 a j_n(k_1 a)]'}{k_1 a} \right\}} = \frac{[k_0 b h_n^{(1)}(k_0 b)]/k_0 b}{k_0 b h_n^{(1)}(k_0 b)}. \quad (14)$$

The characteristic equation is complex and transcendental and the roots of the equation determine the characteristic or resonant frequencies of the modes of oscillation of the dielectric-coated conducting sphere. The complex radian frequency is

$$\omega = \omega' - j\omega'' \quad (15)$$

where ω' gives the free oscillation frequency of the system and $1/\omega''$ gives the relaxation time. Since ω is complex, the propagation constants k_0 and k_1 are also complex, and are given by

$$k_0 = k_0' - jk_0'' = (\omega' - j\omega'') \sqrt{\mu_0 \epsilon_0}$$

$$k_1 = \sqrt{\epsilon_r} k_0.$$

3. Determination of the resonant frequencies

From eqn. (14), the complex resonant frequencies of the dielectric-coated conducting sphere excited in the TM_{ss} mode have been determined. The value $\epsilon_r = 2.56 + j0$ corresponding to the case of perspex has been used for the calculations.

The iterative method was used to determine the resonant frequencies. The real part of the complex frequency was kept fixed at values in the range 1.0 to 20.0 GHz, and the imaginary part was varied from 1.0 to 5.0 GHz.

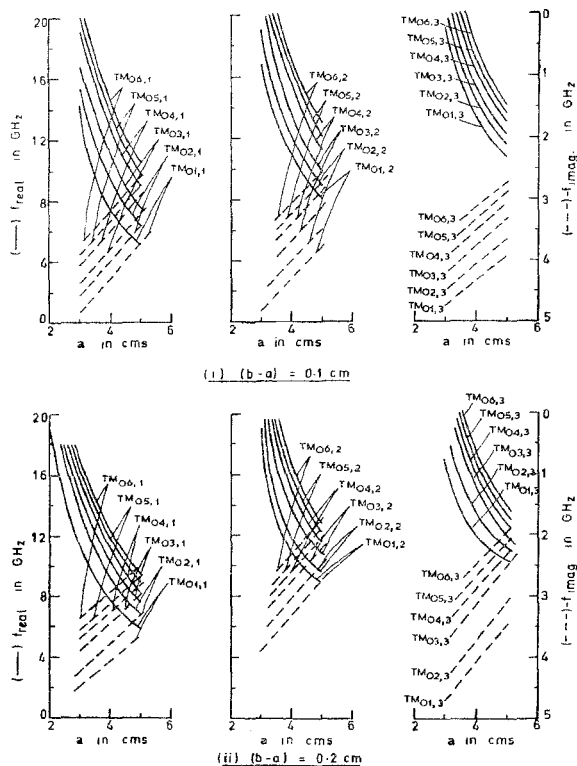


Fig. 1. Variation of the resonant frequency $f_{\text{real}} - jf_{\text{imag.}}$ with inner radius 'a'.

The complex resonant frequencies $f_{\text{real}} - jf_{\text{imag.}} = (\omega' - j\omega'')/2\pi$ of the dielectric-coated conducting sphere have been determined for the values of a varying from 1·0 to 5·0 cm and for values of $(b - a) = 0\cdot1$ cm and $0\cdot2$ cm. The variation of the complex resonant frequency with a for the two cases mentioned above for the $\text{TM}_{sn,s}$ modes, s being the order of the root of the characteristic equation is shown in Fig. 1.

4. Theoretical *Q*-factor of the resonator

The quality factor *Q* of the resonator is defined as 2π times the ratio of the peak energy stored/cycle to the energy dissipated/cycle.

4.1. Peak-energy stored in the resonator

At resonance, the time average electric and magnetic energy stored in the system are equal. The magnetic field component is given by eqn. (5). The peak energy stored in the system is

$$W_s = \frac{\mu}{2} \int_v |H_\phi^s|^2 dv \\ = \mu_0 \pi \left(\frac{k_1}{j\omega \mu_0} \right)^2 \int_{r=a} [L_{on} j_n(k_1 r)]^2 r^2 dr \int_{\theta=0}^{\theta_1} [P'_n(\cos \theta)]^2 \sin \theta d\theta. \quad (16)$$

4.2. Total power radiated

The total power radiated, W_R , is obtained by integrating Poynting's vector over a large sphere which surrounds the dielectric-coated conducting sphere, and is given by

$$W_R = \frac{2\pi}{\eta} \int_{\theta=0}^{\pi} |E_\theta|^2 \sin \theta d\theta \quad (17)$$

where $|E_\theta|$ is the radiation field given by⁶

$$E_\theta = -\frac{j}{2\lambda_0 r} [2\pi b^2 \eta_0 \frac{k_0}{j\omega \mu_0} N_{on} h_n^{(1)}(k_0 b) \exp[j(k_0 r - \omega t)] \\ - [jccs \theta \int_{\theta'=0}^{\theta_1} J_1(k_0 b \sin \theta \sin \theta') \exp(-jk_0 b \cos \theta \cos \theta') \\ P'_n(\cos \theta') \cos \theta' \sin \theta' d\theta' - \sin \theta \int_{\theta'=0}^{\theta_1} J_0(k_0 b \sin \theta \sin \theta') \\ \exp(-jk_0 b \cos \theta \cos \theta') P'_n(\cos \theta') \sin^2 \theta' d\theta']] \\ + 2\pi j b^2 N_{on} [k_0 b h_n^{(1)}(k_0 b)]'/k_0 b \exp[j(k_0 r - \omega t)] \\ \int_{\theta'=0}^{\theta_1} J_1(k_0 b \sin \theta \sin \theta') \exp(-jk_0 b \cos \theta \cos \theta') \\ P'_n(\cos \theta') \sin \theta' d\theta'] \quad (18)$$

4.3. Expression for the *Q*-factor

Using eqns. (16) and (17), we have

$$Q = \omega' \frac{W_s}{W_R}$$

$$\begin{aligned}
&= \omega' \left[\pi \mu_0 \left(\frac{k_1}{j c \mu_1} \right)^2 \int_{r=a}^b [L_{on} j_n(k_1 r) + M_{on} y_n(k_1 r)]^2 r^2 dr \right. \\
&\quad \left. \int_{\theta=0}^{\theta_1} [P'_n(\cos \theta)]^2 \sin \theta d\theta \right] / \frac{2\pi}{\eta} \int_{\theta=0}^{\pi} |E_\theta|^2 \sin \theta d\theta
\end{aligned} \tag{19}$$

Using eqns. (16) and (17), the peak energy stored in the resonator and the total power radiated have been computed at the real resonant frequencies determined above for a few $\text{TM}_{\ell n s}$ modes. The Q of the resonator has been determined using eqn. (19). The results obtained are given in Appendix I.

4.3 Effect of the dielectric losses on the Q -factor

The total power loss in the dielectric, W_L , is given by

$$W_L = \frac{\sigma}{2} \int_v |E^t|^2 dv$$

where σ is the conductivity of the dielectric and $|E^t|$ is the electric field in the dielectric. The electric field components in the dielectric are given by eqns. (3) and (4). From the definition, the Q of the resonator is given by

$$\begin{aligned}
Q &= \frac{\omega' W_S}{W_L + W_R} \\
Q &= \omega' \left[\pi \mu_0 \left(\frac{k_1}{j c \mu_1} \right)^2 \int_{r=a}^b [L_{on} j_n(k_1 r) + M_{on} y_n(k_1 r)]^2 r^2 dr \right. \\
&\quad \left. \int_{\theta=0}^{\theta_1} [P'_n(\cos \theta)]^2 \sin \theta d\theta \right] / \left[\pi \sigma \left[n^2 (n+1)^2 \right. \right. \\
&\quad \left. \left. \int_{r=a}^b \left[(L_{on} + C_{on}) \frac{j_n(k_1 r)}{k_1 r} + (M_{on} + D_{on}) \frac{y_n(k_1 r)}{k_1 r} \right]^2 \right. \right. \\
&\quad \left. \left. r^2 dr \int_{\theta=0}^{\theta_1} [P'_n(\cos \theta)]^2 \sin \theta d\theta \right] + \pi \sigma \left[\int_{r=a}^b \left[(L_{on} + C_{on}) \frac{[k_1 r j_n(k_1 r)]'}{k_1 r} \right. \right. \right. \\
&\quad \left. \left. \left. + M_{on} \frac{[k_1 r y_n(k_1 r)]'}{k_1 r} \right]^2 r^2 dr \int_{\theta=0}^{\theta_1} [P'_n(\cos \theta)]^2 \sin \theta d\theta \right] \right]
\end{aligned}$$

$$+ \frac{2\pi}{\eta} \int_{\theta=0}^{\pi} |E_\theta|^2 \sin \theta d\theta \Big]. \quad (20)$$

The Q of the resonator has been computed using eqn. (20) at the computed real resonant frequencies for a few TM_{om} modes for various dielectric-coated conducting spheres. The results are given in Appendix II.

4.4. Calculation of Q including the reactive energy stored

The Q of the resonator has been calculated by considering the peak energy W_s stored in the field inside the resonator and the peak energy W'_s stored in the reactive field outside⁷. That is, Q is given by

$$Q = \frac{\omega' [W_s + W'_s]}{W_R} \quad (21)$$

where W_s = peak magnetic energy stored in the region $a < r < b$

$$= \frac{\mu}{2} \int_{r=a}^b \int_{\theta=0}^{\theta_1} \int_{\phi=0}^{2\pi} |H_\phi^s|^2 r^2 \sin \theta dr d\theta d\phi$$

W'_s = peak magnetic energy stored in the region $r > b$

$$= \frac{\mu}{2} \int_{r=b}^{r' > b} \int_{\theta=0}^{\pi} \int_{\phi=0}^{2\pi} |H_\phi^s|^2 r^2 \sin \theta dr d\theta d\phi$$

and W_R is given by eqn. (17).

Some of the values are reported in Appendix 3 for the sake of comparison with the Q values calculated earlier at the real resonant frequency ω' by ignoring W'_s .

It is observed that $W'_s (r > b) \ll W_s (a < r < b)$ in practically all the cases and hence the change in the Q values is not significant.

5. Conclusions

The above study leads to the following conclusions:

- (i) The real part of the complex resonant frequency is lower for large values of a and any coating thickness (Fig. 1). Also, the real part of the complex resonant frequency is found to decrease with increase in coating thickness for any particular mode except for a few cases. The imaginary part of the complex resonant frequency is found to increase with increase in a for a particular TM_{om} mode.

(ii) From the values of Q obtained when the dielectric losses are neglected (Appendix I) it is seen that the variation of Q with a is oscillatory for any particular $TM_{on,s}$ mode. The variation of Q for the individual modes is different for different orders of s for both the cases $(b - a) = 0.1$ cm and 0.2 cm considered.

(iii) It is seen that the dielectric loss is of a much smaller magnitude compared to the loss due to radiation in a few cases (Appendix II) and of the same order of magnitude as the total power radiated in some cases (Appendix III). In the first case, the change in the Q values as compared to the case when dielectric losses are neglected is inappreciable and in the latter case, the Q values are much lower than those obtained when dielectric losses are neglected.

The dielectric perspex was considered for the above study. In the case of low loss dielectrics such as teflon or polythene, the dielectric loss will be very small and the energy loss due to radiation will predominate.

(iv) The energy stored in the reactive field is very much less than that stored in the dielectric. Hence there is no significant change in the Q values obtained by considering the reactive energy stored and those obtained by neglecting the stored reactive energy.

(v) A study of the values of the peak energy stored and the total power radiated given in Appendix I shows that they vary in an oscillatory manner for each $TM_{on,s}$ mode with the value of a .

6. Acknowledgement

The authors are grateful to Dr. S. Dhawan, Director of the Indian Institute of Science for providing facilities for the work and to the Council of Scientific and Industrial Research for the sanction of a scheme on this subject.

References

1. GASTINE, M., COURTOIS, L. AND DORMAN, J. L. Electromagnetic resonances of free dielectric spheres, *IEEE Trans.*, 1967, *MTT-15*, pp. 694-700.
2. OKAYA, A. The rutile microwave resonator. *Proc. IRE*, 1960, **48**, 1921.
3. RICHTMEYER, D. Dielectric resonator. *J. Appl. Phys.*, 1939, **10**, 391-398.
4. OKAYA, A. AND BARASH, L. F. The dielectric microwave resonator. *Proc. IRE*, 1962, **50**, 2081-2092.
5. WAHID, P. AND CHATTERJEE, R. The dielectric-coated conducting sphere—modal and near-field characteristics, *Jour. Ind. Inst. Sc.*, 1979, **61** (A), 105-125.
6. WAHID, P. AND CHATTERJEE, R. The truncated dielectric-coated conducting sphere—radiation and gain characteristics, *Jour. Ind. Inst. Sc.*, 1979, **61** (A), 175-194.
7. COLLIN R. E. AND ROTHSCHILD, S. Evaluation of antenna Q' , *IEEE Trans.* 1964, *AP-12*, 23-27.

APPENDIX I

Appendix 1.1: $(b - a) = 0.1$ cm; $\epsilon_r = 2.56$; Mode = $TM_{0n,s}$; s = order of the root of the characteristic equation.

a cm	Mode $TM_{0n,s}$	Characteristic frequency (GHz)	Stored energy W_s (watts)	Total power radiated, W_R (watts)	$Q = \omega' W_s / W_R$
1	2	3	4	5	6
3.0	$TM_{01,1}$	14.3-j4.85	0.1649×10^{-13}	0.6832×10^{-5}	0.217×10^3
	$TM_{01,2}$	16.7-j4.80	0.9643×10^{-14}	0.9505×10^{-6}	0.106×10^4
	$TM_{01,3}$	19.1-j4.7	0.6198×10^{-12}	0.5033	0.148
	$TM_{02,1}$	15.0-j4.6	0.2782×10^{-14}	0.6751×10^{-5}	0.388
	$TM_{02,2}$	19.1-j4.55	0.1616×10^{-8}	0.3699×10^{-2}	0.525×10^5
	$TM_{03,1}$	16.7-j4.3	0.4563×10^{-14}	0.2976×10^{-2}	0.160
	$TM_{03,2}$	19.9-j4.25	0.1919×10^{-12}	0.5513×10^{-3}	0.435×10^2
	$TM_{04,1}$	19.3-j4.10	0.3487×10^{-15}	0.7944×10^{-4}	0.532
3.5	$TM_{01,1}$	9.5-j4.55	0.5595×10^{-14}	0.1125×10^{-5}	0.296×10^3
	$TM_{01,2}$	13.0-j4.55	0.1614×10^{-14}	0.1208×10^{-3}	0.109×10^4
	$TM_{01,3}$	15.6-j4.80	0.3371×10^{-15}	0.9535×10^{-5}	0.347×10^1
	$TM_{02,1}$	11.8-j4.3	0.1173×10^{-14}	0.6633×10^{-1}	0.131×10^1
	$TM_{02,2}$	14.8-j4.3	0.1131×10^{-14}	0.3164×10^{-2}	0.332×10^{-1}
	$TM_{02,3}$	16.4-j4.25	0.8971×10^{-15}	0.1789×10^{-1}	0.516
	$TM_{03,1}$	13.8-j4.05	0.4056×10^{-15}	0.1949×10^{-5}	0.180
	$TM_{03,2}$	16.8-3.95	0.6463×10^{-13}	0.2718	0.251×10^{-1}
4.0	$TM_{03,3}$	17.4-j4.0	0.6164×10^{-14}	0.3687×10^{-1}	0.183×10^{-1}
	$TM_{01,1}$	7.1-j4.3	0.4959×10^{-15}	0.3802×10^{-6}	0.581×10^3
	$TM_{01,2}$	10.8-j4.6	0.1053×10^{-13}	0.6898×10^{-4}	0.104×10^2
	$TM_{01,3}$	13.4-j4.25	0.6196×10^{-13}	0.1524×10^{-1}	0.342
	$TM_{02,1}$	9.5-j4.10	0.2969×10^{-14}	0.1321×10^{-4}	0.128×10^2
	$TM_{02,2}$	12.0-j4.0	0.4413×10^{-14}	0.4253×10^{-2}	0.782×10^{-1}
	$TM_{02,3}$	14.3-j4.0	0.1923×10^{-11}	0.1118×10^1	0.155
	$TM_{03,1}$	11.5-j3.75	0.8613×10^{-15}	0.6508×10^{-8}	0.957×10^{-1}
4.5	$TM_{03,2}$	14.3-j3.70	0.5252×10^{-15}	0.9478×10^{-1}	0.505×10^{-1}
	$TM_{03,3}$	15.0-j3.75	0.2171×10^{-12}	0.2444×10^{-1}	0.836
	$TM_{04,1}$	13.2-j3.05	0.8717×10^{-15}	0.3262×10^{-4}	0.221×10^1
	$TM_{04,2}$	16.0-j3.50	0.3035×10^{-15}	0.1043×10^{-4}	0.292×10^1
	$TM_{04,3}$	16.7-j3.55	0.2115×10^{-13}	0.6212×10^{-8}	0.357×10^1
	$TM_{05,1}$	6.2-j3.95	0.1594×10^{-15}	0.2073×10^{-3}	0.298×10^4
	$TM_{05,2}$	9.4-j4.0	0.1518×10^{-15}	0.2877×10^{-6}	0.312×10^4
	$TM_{05,3}$	11.8-j4.15	0.1198×10^{-12}	0.3144×10^{-2}	0.282×10^1
$a = 0.1$ cm	$TM_{06,1}$	7.8-j5.2	0.4139×10^{-15}	0.1128×10^{-6}	0.179×10^4
	$TM_{06,2}$	10.3-j3.75	0.5131×10^{-14}	0.1109×10^{-2}	0.299×10^1
	$TM_{06,3}$	12.8-j3.85	0.2345×10^{-11}	0.1465	0.129×10^1
	$TM_{07,1}$	9.0-3.7	0.1633×10^{-15}	0.7202×10^{-5}	0.128×10^3

1	2	3	4	5	6
TM _{03,2}	11·4-j3·35	0·9452 × 10 ⁻¹³	0·6299 × 10 ⁻²	0·108 × 10 ¹	
TM _{03,3}	13·6-j3·5	0·3288 × 10 ⁻¹⁴	0·6542 × 10 ⁻²	0·429	
TM _{04,1}	10·6-j3·2	0·8693 × 10 ⁻¹⁸	0·4287 × 10 ⁻⁷	0·135 × 10 ¹	
TM _{04,2}	13·2-j3·1	0·9274 × 10 ⁻¹⁵	0·4029 × 10 ⁻³	0·191	
TM _{04,3}	14·6-j3·25	0·4213 × 10 ⁻¹⁵	0·3121 × 10 ⁻¹	0·124 × 10 ¹	
5·0	TM _{01,1}	5·2-j3·75	0·5150 × 10 ⁻¹⁵	0·1169 × 10 ⁻⁶	0·201 × 10 ³
	TM _{01,2}	8·0-j3·75	0·1174 × 10 ⁻¹⁴	0·1487 × 10 ⁻⁵	0·629 × 10 ²
	TM _{01,3}	10·6-j3·8	0·2879 × 10 ⁻¹³	0·5414 × 10 ⁻¹	0·354 × 10 ⁻¹
	TM _{02,1}	6·5-j3·3	0·2942 × 10 ⁻¹⁵	0·7581 × 10 ⁻⁷	0·158 × 10 ³
	TM _{02,2}	8·8-j3·5	0·4251 × 10 ⁻¹⁵	0·1473 × 10 ⁻³	0·159
	TM _{02,3}	11·6-j3·55	0·6757 × 10 ⁻¹²	0·2065	0·238
	TM _{03,1}	7·1-j3·20	0·1441 × 10 ⁻¹⁸	0·8960 × 10 ⁻⁶	0·717 × 10 ¹
	TM _{03,2}	9·8-j3·15	0·3157 × 10 ⁻¹⁶	0·8821 × 10 ⁻⁴	0·188
	TM _{03,3}	12·2-j3·35	0·4649 × 10 ⁻¹³	0·4744 × 10 ⁻³	0·750 × 10 ²
	TM _{04,1}	9·0-j3·01	0·2153 × 10 ⁻¹⁵	0·5479 × 10 ⁻⁶	0·222 × 10 ²
	TM _{04,2}	11·0-j2·9	0·5608 × 10 ⁻¹⁷	0·5750 × 10 ⁻⁶	0·674 × 10 ¹
	TM _{04,3}	13·0-j3·15	0·6325 × 10 ⁻¹⁶	0·7534 × 10 ⁻³	0·545

Appendix 1.2.: $(b - a) = 0.2 \text{ cm}$; $\epsilon_r = 2.56$; Mode = TM_{0n,s}; s = order of the root of the characteristic equation.

1	2	3	4	5	6
2·0	TM _{01,1}	19·1-j4·8	0·2401 × 10 ⁻¹³	0·2821 × 10 ⁻²	0·102 × 10 ¹
3·0	TM _{01,1}	12·0-j4·67	0·7372 × 10 ⁻¹⁴	0·7559 × 10 ⁻³	0·735
	TM _{01,2}	19·1-j3·90	0·3143 × 10 ⁻¹²	0·5936 × 10 ⁻¹	0·635 × 10 ¹
	TM _{02,1}	14·3-j4·3	0·7223 × 10 ⁻¹⁴	0·4719 × 10 ⁻³	0·137 × 10 ¹
	TM _{02,2}	15·5-j4·0	0·1955 × 10 ⁻¹³	0·1673 × 10 ⁻²	0·114 × 10 ¹
3·5	TM _{01,1}	9·2-j4·25	0·2594 × 10 ⁻¹³	0·1884 × 10 ⁻⁴	0·796 × 10 ²
	TM _{01,2}	12·8-j3·65	0·3413 × 10 ⁻¹⁴	0·1058 × 10 ⁻²	0·259
	TM _{01,3}	13·7-j4·4	0·4041 × 10 ⁻¹⁴	0·1384 × 10 ⁻³	0·251 × 10 ¹
	TM _{02,1}	11·1-j4·0	0·3679 × 10 ⁻¹³	0·1549 × 10 ⁻²	0·166 × 10 ¹
	TM _{02,2}	14·2-j3·3	0·9506 × 10 ⁻¹²	0·3767 × 10 ⁻²	0·225
	TM _{02,3}	15·8-j4·1	0·3189 × 10 ⁻¹²	0·3567 × 10 ⁻¹	0·887
	TM _{03,1}	12·3-j3·7	0·2747 × 10 ⁻¹⁴	0·6921 × 10 ⁻⁴	0·307 × 10 ¹
	TM _{03,2}	16·5-j3·0	0·1499 × 10 ⁻¹¹	0·1583	0·982
	TM _{03,3}	18·0-j3·1	0·7204 × 10 ⁻¹⁶	0·1745 × 10 ⁻²	0·467 × 10 ⁻¹

1	2	3	4	5	6
4·0	TM _{01z1}	7·5-j4·5	0·3828 × 10 ⁻¹³	0·9991 × 10 ⁻⁴	0·181 × 10 ²
	TM _{01z2}	10·6-j3·2	0·3602 × 10 ⁻¹³	0·7234 × 10 ⁻⁴	0·329 × 10 ²
	TM _{01z3}	11·9-j4·5	0·7828 × 10 ⁻¹³	0·1114 × 10 ⁻¹	0·525 × 10 ³
	TM _{02z1}	9·5-j3·7	0·1775 × 10 ⁻¹³	0·5238 × 10 ⁻³	0·202 × 10 ¹
	TM _{02z2}	12·0-j3·0	0·3334 × 10 ⁻¹³	0·3387 × 10 ⁻¹	0·741 × 10 ⁻¹
	TM _{02z3}	14·3-j3·8	0·8179 × 10 ⁻¹¹	0·5259 × 10 ⁻¹	0·391 × 10 ²
	TM _{03z1}	10·2-j2·95	0·3319 × 10 ⁻¹³	0·3851 × 10 ⁻³	0·552 × 10 ¹
	TM _{03z2}	14·1-j2·7	0·4554 × 10 ⁻¹³	0·8236 × 10 ⁻¹	0·489 × 10 ¹
	TM _{03z3}	16·3-j3·3	0·5231 × 10 ⁻¹¹	0·1214 × 10 ¹	0·441
4·5	TM _{01z1}	6·6-j3·85	0·2820 × 10 ⁻¹³	0·7777 × 10 ⁻⁴	0·150 × 10 ²
	TM _{01z2}	9·8-j3·05	0·2503 × 10 ⁻¹⁴	0·3377 × 10 ⁻³	0·470
	TM _{01z3}	11·1-j3·80	0·1054 × 10 ⁻¹²	0·1323 × 10 ⁻³	0·557
	TM _{02z1}	7·8-j3·5	0·1254 × 10 ⁻¹³	0·1657 × 10 ⁻³	0·369
	TM _{02z2}	10·6-j2·75	0·1899 × 10 ⁻¹³	0·3419 × 10 ⁻¹	0·371
	TM _{02z3}	12·2-j3·4	0·1120 × 10 ⁻¹²	0·1809	0·476 × 10 ⁻¹
	TM _{03z1}	8·9-j3·2	0·3630 × 10 ⁻¹³	0·2879 × 10 ⁻³	0·721 × 10 ¹
	TM _{03z2}	12·1-j2·45	0·3659 × 10 ⁻¹²	0·3135 × 10 ⁻²	0·887 × 10 ¹
	TM _{03z3}	13·5-j2·85	0·3358 × 10 ⁻¹³	0·1753 × 10 ⁻¹	0·163 × 10 ⁻²
5·0	TM _{01z1}	5·9-j3·6	0·2065 × 10 ⁻¹³	0·5617 × 10 ⁻⁴	0·136 × 10 ²
	TM _{01z2}	9·2-j2·7	0·4357 × 10 ⁻¹⁴	0·4480 × 10 ⁻³	0·561
	TM _{01z3}	10·4-j3·5	0·6721 × 10 ⁻¹⁴	0·5329 × 10 ⁻³	0·824
	TM _{02z1}	6·5-j3·2	0·3466 × 10 ⁻¹⁴	0·1685 × 10 ⁻⁴	0·839 × 10 ¹
	TM _{02z2}	9·6-j2·45	0·4344 × 10 ⁻¹⁴	0·9924 × 10 ⁻³	0·264
	TM _{02z3}	11·3-j3·05	0·3933 × 10 ⁻¹¹	0·3578 × 10 ¹	0·281 × 10 ³
	TM _{03z1}	7·1-j2·95	0·8776 × 10 ⁻¹³	0·1173 × 10 ⁻³	0·333
	TM _{03z2}	11·0-j2·25	0·8727 × 10 ⁻¹³	0·1983 × 10 ⁻¹	0·304
	TM _{03z3}	12·1-j2·5	0·2522 × 10 ⁻¹¹	0·5802 × 10 ⁻¹	0·330 × 10 ¹

APPENDIX II

Appendix 2.1

<i>a</i>	<i>b</i>	Mode $TM_{0n,s}$	Characteristic frequency (GHz)	Stored energy, W_s (watts)	Dielectric loss, W_L (watts)	Total power radiated, W_R (watts)	Q	$\frac{\omega' W_s}{W_L + W_R}$	$Q = \omega' W_s/W_R$ (from Table I)
1	2	3	4	5	6	7	8	9	
3.0	3.1	$TM_{01,s}$	$19.1-j4.7$	0.6198×10^{-12}	0.2426×10^{-2}	0.5033	0.147	0.148	
		$TM_{03,1}$	$16.7-j4.3$	0.4563×10^{-11}	0.1531×10^{-3}	0.2796×10^{-2}	0.160	0.160	
4.0	4.1	$TM_{01,3}$	$13.4-j4.25$	0.6196×10^{-13}	0.4424×10^{-5}	0.1524×10^{-1}	0.342	0.342	
		$TM_{02,3}$	$14.3-j4.0$	0.1923×10^{-11}	0.7937×10^{-4}	0.1118×10^1	0.155	0.155	
5.0	5.1	$TM_{01,3}$	$10.6-j3.8$	0.2879×10^{-13}	0.9728×10^{-6}	0.5414×10^{-1}	0.354×10^{-1}	0.354×10^{-1}	
		$TM_{02,3}$	$11.6-j3.65$	0.6757×10^{-12}	0.5586×10^{-3}	0.2065	0.378	0.378	
3.0	3.2	$TM_{00,1}$	$15.5-j4.0$	0.1955×10^{-13}	0.2258×10^{-4}	0.1673×10^{-2}	0.112×10^1	0.114×10^1	
4.0	4.2	$TM_{00,2}$	$12.0-j3.0$	0.3334×10^{-13}	0.1985×10^{-4}	0.3389×10^{-1}	0.742×10^{-1}	0.747×10^{-1}	
		$TM_{03,2}$	$14.1-j2.7$	0.4554×10^{-13}	0.5258×10^{-6}	0.8236×10^{-1}	0.613×10^{-1}	0.489×10^1	
		$TM_{02,3}$	$16.3-j3.3$	0.5231×10^{-11}	0.4369×10^{-2}	0.1214×10^1	0.441	0.441	
5.0	5.2	$TM_{02,3}$	$11.3-j3.05$	0.3933×10^{-11}	0.2529×10^{-3}	0.3578×10^1	0.780×10^{-1}	0.281×10^3	
		$TM_{02,2}$	$11.0-j2.25$	0.8727×10^{-13}	0.2393×10^{-4}	0.1983×10^{-1}	0.304	0.204	

Appendix 2.2

<i>a</i>	<i>b</i>	Mode $TM_{0n,s}$	Characteristic frequency (GHz)	Stored energy, W_s (watts)	Dielectric loss, W_L (watts)	Total power radiated, W_R (watts)	$Q = \frac{\omega' W_s}{W_L + W_R}$	$Q = \omega' W_s/W_R$ (from Table I)
1	2	3	4	5	6	7	8	9
3.0	3.1	$TM_{01,1}$	$14.3-j4.83$	0.1649×10^{-13}	0.7485×10^{-6}	0.6832×10^{-5}	0.104×10^3	0.217×10^3
		$TM_{03,2}$	$19.9-j4.25$	0.1919×10^{-12}	0.1791×10^{-3}	0.5513×10^{-3}	0.328×10^2	0.435×10^2

4·0	4·1	$TM_{01,1}$	$9\cdot5-j4\cdot10$	$0\cdot2969 \times 10^{-14}$	$0\cdot2322 \times 10^{-4}$	$0\cdot1321 \times 10^{-4}$	$0\cdot486 \times 10^1$	$0\cdot128 \times 10^2$
		$TM_{02,1}$	$11\cdot5-j3\cdot75$	$0\cdot8613 \times 10^{-16}$	$0\cdot5239 \times 10^{-6}$	$0\cdot6508 \times 10^{-6}$	$0\cdot529 \times 10^1$	$0\cdot957 \times 10^1$
5·0	5·1	$TM_{01,2}$	$8\cdot0-j3\cdot75$	$0\cdot1174 \times 10^{-14}$	$0\cdot4819 \times 10^{-6}$	$0\cdot1487 \times 10^{-6}$	$0\cdot936 \times 10^1$	$0\cdot629 \times 10^2$
		$TM_{02,3}$	$12\cdot2-j3\cdot35$	$0\cdot4649 \times 10^{-12}$	$0\cdot2336 \times 10^{-8}$	$0\cdot4744 \times 10^{-8}$	$0\cdot502 \times 10^2$	$0\cdot750 \times 10^2$
3·0	3·2	$TM_{01,3}$	$19\cdot1-j3\cdot90$	$0\cdot3143 \times 10^{-12}$	$0\cdot1379 \times 10^{-1}$	$0\cdot5936 \times 10^{-1}$	$0\cdot516 \times 10^{-1}$	$0\cdot635 \times 10^{-1}$
4·0	4·2	$TM_{01,2}$	$10\cdot6-j3\cdot2$	$0\cdot3602 \times 10^{-13}$	$0\cdot2407 \times 10^{-4}$	$0\cdot7234 \times 10^{-4}$	$0\cdot249 \times 10^2$	$0\cdot329 \times 10^2$
		$TM_{01,3}$	$11\cdot9-j4\cdot5$	$0\cdot7828 \times 10^{-13}$	$0\cdot3512 \times 10^{-4}$	$0\cdot1114 \times 10^{-4}$	$0\cdot127 \times 10^2$	$0\cdot525 \times 10^2$
5·0	5·2	$TM_{02,1}$	$6\cdot5-j3\cdot2$	$0\cdot3466 \times 10^{-14}$	$0\cdot1144 \times 10^{-4}$	$0\cdot6685 \times 10^{-4}$	$0\cdot501 \times 10^1$	$0\cdot839 \times 10^1$

APPENDIX III

a cm	b cm	Mode $TM_{0n,1}$	Real frequency ω'	Peak energy stored (watts)		Total power radiated W_R (watts)	$Q = \frac{\omega' (W_s + W'_s)}{W_R}$	$Q = \omega' W_s / W_R$ (from Table I)
				W_s	W'_s			
3·0	3·1	$TM_{01,1}$	$0\cdot1049 \times 10^{12}$	$0\cdot4563 \times 10^{-14}$	$0\cdot7026 \times 10^{-16}$	$0\cdot2976 \times 10^{-2}$	0·161	0·161
4·0	4·1	$TM_{02,2}$	$0\cdot7539 \times 10^{11}$	$0\cdot4413 \times 10^{-14}$	$0\cdot4953 \times 10^{-18}$	$0\cdot4253 \times 10^{-2}$	$0\cdot782 \times 10^{-1}$	$0\cdot782 \times 10^{-1}$
5·0	5·1	$TM_{02,3}$	$0\cdot7286 \times 10^{11}$	$0\cdot6757 \times 10^{-12}$	$0\cdot3412 \times 10^{-17}$	0·2065	0·338	0·338
4·5	4·7	$TM_{03,2}$	$0\cdot6660 \times 10^{11}$	$0\cdot1899 \times 10^{-13}$	$0\cdot9862 \times 10^{-17}$	$0\cdot3419 \times 10^{-4}$	0·371	0·371
5·0	5·2	$TM_{03,1}$	$0\cdot4461 \times 10^{11}$	$0\cdot8776 \times 10^{-15}$	$0\cdot1229 \times 10^{-18}$	$0\cdot1173 \times 10^{-5}$	0·334	0·334